Hindawi Publishing Corporation
International Journal of Geophysics
Volume 2013, Article ID 608037, 12 pages
http://dx.doi.org/10.1155/2013/608037

Review Article

Sensitivity and Resolution Capacity of Electrode Configurations

Cyril Chibueze Okpoli

Department of Geology and Applied Geophysics, Faculty of Science, Adekunle Ajasin University, PMB 001, Akungba-Akoko, Ondo State, Nigeria

Correspondence should be addressed to Cyril Chibueze Okpoli; okpolicyril@gmail.com

Received 10 June 2013; Revised 26 July 2013; Accepted 25 August 2013

Academic Editor: Francesco Soldovieri

This paper reviews the geological conditions, data density, and acquisition geometry that have direct influence on the sensitivity and resolution capacity of several electrode configurations. The parameters appreciate the effectiveness of automated multichannel system which has evolved several electrode arrays that are cost effective, reduction in survey time, high sensitivity, and resolution capacity in 2D and 3D resistivity tomographies. The arrays are pole-pole, pole-dipole, pole-bipole, dipole-dipole, Wenner, Wenner-β, γ, gradient, midpoint-potential-referred, Schlumberger, square, and Lee-partition arrays. The gradient array and midpoint-potential-referred are well suited for multichannel surveying and gradient array images are comparable to dipole-dipole and pole-dipole. 2D electrical resistivity surveys can produce out-of-plane anomaly of the subsurface which could be misleading in the interpretation of subsurface features. Hence, a 3D interpretation model should give more accurate results, because of the increase in the reliability of inversion images and complete elimination of spurious features. Therefore, the reduction of anomaly effects and damping factor due to signal to noise ratio result in better spatial resolution image, thus enhancing its usage in environmental and engineering research.

1. Introduction

Most targets of environmental and engineering interest are at shallow depths. Geophysical responses from near-surface sources usually treated as noise in traditional geophysical exploration surveys are often the targets of interest in environmental and engineering investigations. The subsurface geology can be complex, subtle, and multiscale such that spatial variations can change rapidly both laterally and vertically. Thus, a closely spaced grid of observation points is required for their accurate characterization, high spatial resolution of the anomaly, and good target definition. Survey design in geoelectrical resistivity surveys must take into account the capabilities of the data acquisition system, heterogeneities of the subsurface electrical resistivities, and the resolution required. Other factors to be considered are the area extent of the site to be investigated, the cost of the survey, and the time required to complete the survey [1].

Geoelectrical surveys were introduced by Conrad Schlumberger and Marcel Schlumberger in 1932 and have subsequently been investigated by many researchers for numerous electrode configurations and subsurface structures. This concept has been used in the qualitative comparison of the effective responses of different electrode arrays and in the general understanding of the subsurface origin of observed apparent resistivity [2]. Early attempts assumed that the depth of investigation solely depends on the depth of current penetration, which is a function of the current electrodes separation. For example, [3] presented computations of two- and three-layer earth models by considering only the current electrodes separation.

The depth of investigation has been defined as the depth at which a thin horizontal layer makes the maximum contribution to the total observed signal at the surface [4]. This definition was used by [5, 6] to compute characteristic curves for various conventional electrode arrays over a homogeneous isotropic medium showing the response of a thin horizontal layer with varying depth. The point where these "depth of investigation characteristic" (DIC) curves attain a maximum defines the depth of investigation of the electrode array. The theoretical basis [6], supported by [7], for Roy and Apparao's research work has been strongly criticized [8, 9]. However, [10] demonstrated, using a boundary value approach, that the relationships developed by [5] are correct for a homogeneous

earth model which provides a general case useful for electrical resistivity investigations. The practical usefulness and validity of these relationships have been discussed by [11, 12].

A more practical and useful value for the depth of investigation may be provided by the median value of Roy and Apparao's normalized DIC curves and not the maximum [13, 14]. This median depth measure is referred to as the effective depth of investigation. It is the depth at which the total of one-half of the signal originates from above and the other half from below. In both definitions, the depth of investigation practically depends on the relative positions of both the current and potential electrodes and not on the depth of current penetration only, which is determined by the current electrode separation. Another factor that influences the depth of investigation is the measurability of the signal by the measuring equipment. The ability of the equipment to detect the amplitude of the signal and of the existing noise, the power specification of the equipment, and its ability to filter noise all affect the depth of investigation. The depth of investigation also depends on the subsurface layering [14]; a low-resistivity surface layer reduces the depth of investigation.

In electrical resistivity field observations, four electrodes are generally placed at arbitrary locations. However, a number of electrode configurations have been used in recording resistivity field data, each suitable for a particular geological situation with varying anomaly resolution. The conventional arrays most commonly used include the conventional Wenner (Wenner-alpha), Schlumberger, dipole-dipole, pole-pole, and pole-dipole arrays. Other variants of the conventional Wenner array are Wenner-beta, Wenner-gamma, and Wenner-Schlumberger arrays [15, 16] and are illustrated in Figure 1. Wenner-Schlumberger array is a hybrid between the Wenner-alpha and Schlumberger arrays [17]. It is a digitized form of the Schlumberger array that allows it to be used on automated multielectrode systems with constant electrode spacing. The Wenner-beta array is a special case of dipole-dipole array with the n-factor equal to one. In Wenner-gamma array, the current and the potential electrodes are interleaved.

The apparent resistivity values observed by the different array types over the same structure can be very different. The choice of a particular array depends on a number of factors, which include the geological structures to be delineated, heterogeneities of the subsurface, anomaly resolution of the array, sensitivity of the resistivity meter, the background noise level, and electromagnetic coupling. Other factors to be considered are the sensitivity of the array to vertical and lateral variations in the resistivity of the subsurface, its depth of investigation, and the horizontal data coverage and signal strength of the array [18].

These measurements sets include every possible conventional and nonconventional electrode arrays. Surveys with this suite of electrode configurations result in comprehensive data sets which would contain all resistivity subsurface information that the n-electrodes system is capable of gathering. However, a large portion of these configurations have large geometric factors and are capable of reducing the stability of the inversion of the observed data sets. The works of [19] assessed the imaging potential of data sets acquired with modern multielectrode resistivity systems using synthetic and field examples. They showed that comprehensive data sets recorded with large numbers of four-point electrode configurations provide significantly more information than those with standard electrode arrays. However, the recording of comprehensive data sets requires too many measurements and is not cost effective in routine geoelectrical resistivity surveys.

An optimization procedure that utilizes a goodness function that ranks the sensitivities of all electrode configurations can be used to define suite of electrode configurations that yields images comparable in quality to comprehensive images [20–22]. The goodness function includes weighting terms which counterbalance the high sensitivities of the model relative to deeper parts and minimize the influence of well resolved regions of the model based on the experimental design procedure. Data generated with electrode configurations that yields large amounts of new information according to their high sensitivities and depth of influence are incorporated into the successively increasing optimal data sets.

Many electrode configurations such as pole-pole, pole-dipole, pole-bipole, Wenner, Schlumberger, dipole-dipole, Wenner-β and -γ array have been used in electric exploration. Pole-bipole is a special case of pole-dipole with n-factor equal to one; Wenner-beta is special case of dipole-dipole and Wenner of Schlumberger as well as gradient array and mid-potential-referred measurement. They have their advantages and limitations in fieldwork but provide useful practical applicability for surface sounding, profiling for 2D and 3D tomographies that is, pole-pole, Schlumberger, pole-dipole, and dipole-dipole [23, 24]. In practice it is always difficult to acquire data in pole-pole due to limited access to remote electrodes and sometimes a long potential reference electrode layout may pick up noise. The sensitivities and abilities of the several electrode configurations in relation to their differences in spatial resolution, tendency for artefacts to appear in images, deviation from the true model resistivity and interpretable maximum depth are limitations usually encountered in fieldwork.

Author in [25] compared the resolution of crosshole tomography with pole-pole, pole-dipole, and dipole-dipole arrays and he suggested that dipole-dipole surveying, when the instrument is high, is more suitable for resolving complex structures than pole-pole array, and pole-dipole may be a good compromise between resolution and signal strength.

The reliability and resolution capacity of Wenner array as examined by [26, 27], pointed out that Wenner data density is important and that the inverted model provides approximate guide to the true geometry and true formation resistivity. In order to get a high resolution and reliable image, multielectrode cable with a fixed interelectrode spacing is usually utilized to capture maximum anomaly information, reasonable data coverage, and high signal noise ratio. Consecutive usage of a and n in a theoretical complete data set of arrays with low noise contamination is essential in obtaining high-resolution image but increases the fieldwork time.

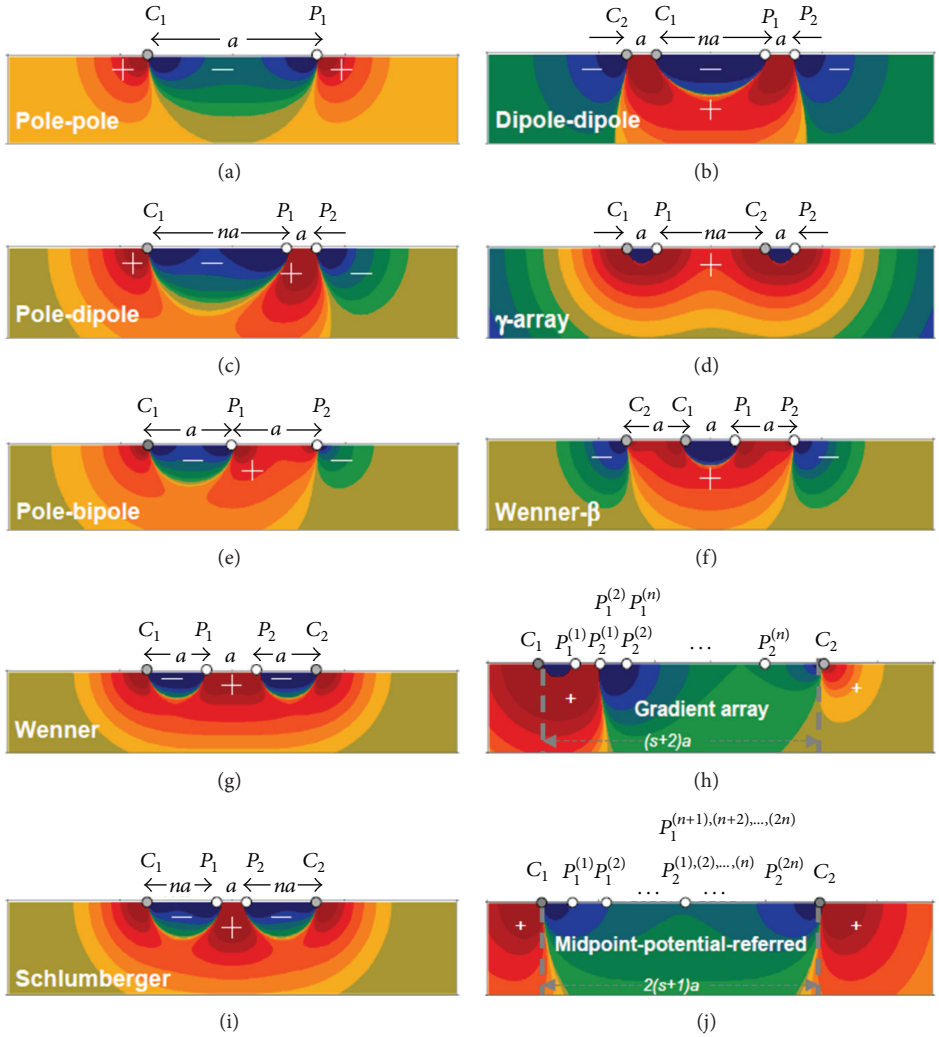

FIGURE 1: Sensitivity and resolution diagrams of electrode configurations. (a) Pole-pole, (b) dipole-dipole, (c) pole-dipole, (d) γ-array, (e) pole-bipole, (f) Wenner-β, (g) Wenner, (h) gradient array, (i) Schlumberger, and (j) midpoint-potential-referred [15].

In all the electrode arrays larger spacing of a and n gives deeper information about the subsurface, while small spacing of a and n probably offers a relatively good horizontal resolution for the shallower sections of the ground.

The effectiveness of different electrode arrays in estimation of anomaly effects was developed by [28] which are significantly larger than background noise from the imaging perspective.

The square array was originally developed as an alternative to Wenner or Schlumberger arrays when a dipping subsurface, bedding, or foliation was present [29]. Techniques for analyzing directional-resistivity data provided by the square-array method have been developed [30], but the method has not been widely used. Few case studies or interpretive methods specifically applied to the square array are found in the literature, although commercial software is available for layered earth interpretations.

The square array is more sensitive to a given rock heterogeneity and anisotropy than the more commonly used Schlumberger and Wenner arrays. Thus, it is advantageous over equivalent survey using a Schlumberger or Wenner array in that it requires about 65 percent less surface area.

Field measurement in the square-array method is conducted in a manner similar to that for traditional collinear arrays. The location of a measurement is assigned to the center point of the square. The array size (A) is the length of the side of the square. The array is expanded symmetrically about the centerpoint, in increments of $A(2)^{1/2}$ [29], so that the sounding can be interpreted as a function of depth.

For each square, three measurements are made—two perpendicular measurements (alpha, a; and beta, b) and one diagonal measurement (gamma, g) (Figure 2). The a and b measurements provide information on the directional variation of the subsurface apparent resistivity (r_a). The azimuthal

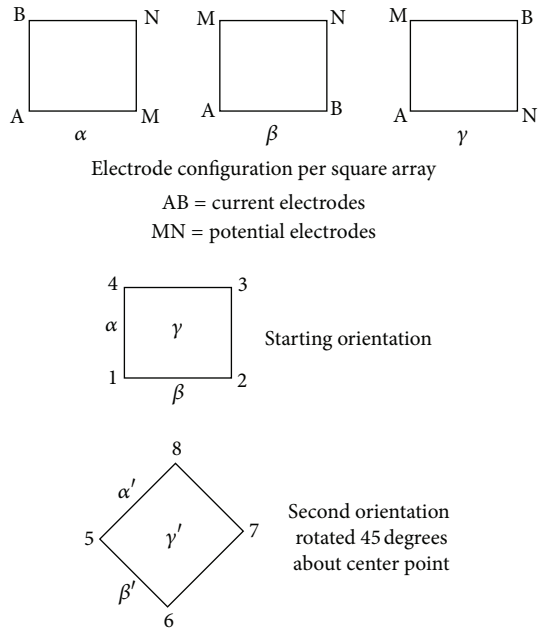

Figure 2: Electrode configuration for square array.

orientation of the a and b measurements is that of the line connecting the current electrodes. The g measurement serves as a check on the accuracy of the a and b measurements.

In Figure 3, Lee-partition array is the same as the Wenner array, except that an additional potential electrode 0 is placed at the centre of the array between the potential electrodes M and N. Measurements of the potential difference are made between 0 and M and between 0 and N. The formula for computing the Lee-partitioning apparent resistivity is given by

$$\overline{\rho}_{\text{L.P.}} = 4\pi a \frac{\Delta V}{I}, \tag{1}$$

where ΔV is the potential difference between 0 and M or 0 and N. This array I has been used extensively in the past [31].

2. Sensitivity Function

Sensitivity is a reasonable quantity in electrical resistivity data interpretation process. It captures the changes in the potential due to changes in resistivity of a cell volume. For inversion schemes, the sensitivity provides a link between the observed data and the model vector in terms of the Jacobian matrix and is useful for the interpretation of field data employing forward modelling. Thus, the resolvability of the model parameters can be assessed using sensitivity [32]. Sensitivity studies are usually carried out in conjunction with inversion techniques. [33] depict the sensitivity, as an example, for a single pole source at the surface for 1D and 2D cases and show the distortion of the sensitivity for a 2D prismatic body. Frechet derivatives are deduce by [34] in the sense of single scattering theory and they compared their evolved DC expression with the one for a 1D earth model described by [35]. The presentation of a coarse 3D sensitivity plot is done by [36] for a surface dipole-dipole configuration using two orthogonal sectors through 3D space. A vertical section of the dipole-dipole arrangement at the surface was also presented by [37], while [38] carried out sensitivity study using small 3D grids. [39] has presented four ways in which the sensitivity of three-dimensional bodies can be computed. These techniques include an analytical solution for a homogeneous half-space and three numerical approaches for arbitrary resistivity structures which include DC forward modelling using a source at the transmitter and a fictitious source at the receiver location; finite difference approach solving a set of partial differential equations defining the sensitivity problem; and a two DC forward runs employing perturbation of a resistivity block to derive the sensitivity.

The depth of investigation of an array can be assessed quantitatively by using sensitivity function, which is given by the Frechet derivative [33]. The sensitivity function of an array indicates the degree to which the variations in resistivity of a section of the subsurface will influence the potential measured by the array. Higher values of the sensitivity function show greater influence of the subsurface region on the measurements. The sensitivity functions of several electrode configurations over homogeneous and layered earth models are presented by [39]. For a given source and receiver configuration of electrodes, the sensitivity function S is expressed as the inner product of the current densities $\vec{J}_S$ and $\vec{J}_R$ produced by a current source of strength I at the source and receiver positions, respectively, integrated over the perturbed volume dV:

$$S = \frac{\Delta\Phi}{\Delta\rho} = \frac{1}{I} \int_v \vec{J}_S \cdot \vec{J}_R dV. \tag{2}$$

3. Fundamental Theory of Electrical Resistivity Surveys

Electrical and electromagnetic (EM) methods are essential tools in the field of applied geophysics for about a century, particularly for shallow and near-surface investigations. These geophysical prospecting methods are defined by their frequency of operation, the origin of the source signals, and the manner by which the sources and receivers are coupled to the ground. The signal frequencies range from a few hertz (Hz) in direct-current (DC) resistivity surveys up to several gigahertz (GHz) in ground-penetrating radar (GPR) measurements. The methods are generally governed by Maxwell's equations of electromagnetism [40–43]. Wave propagation dominates at high frequencies, whereas diffusion is the

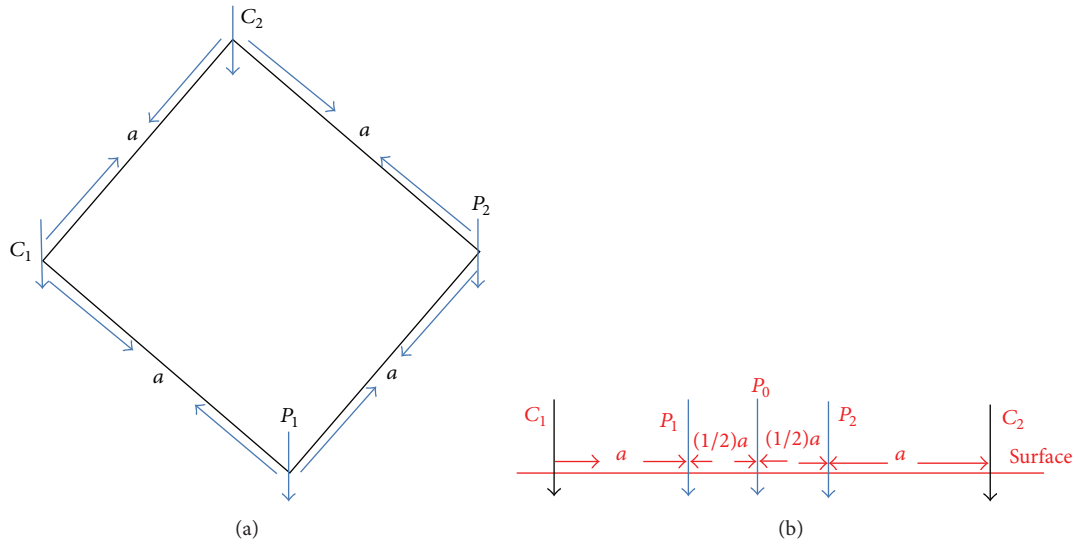

Figure 3: Schematic diagrams of electrode configurations. (a) Square array, (b) Lee-partition.

dominant physical mechanism of electromagnetic induction at lower frequencies (in the quasistatic 16 approximation). In the direct-current (DC) frequency, the diffusion term is zero and the field is thus governed entirely by Poisson's equation.

Electrical and electromagnetic methods may either be passive or active. Passive methods use electromagnetic (EM) fields created by natural phenomena as source signals (e.g., telluric currents) while active methods employ signal generators to generate the required input signals. Sources and receivers can be coupled to the ground through galvanic contacts such as planted electrodes or through EM induction such as coils of wire. These possibilities result in a greater variety of field techniques than any other geophysical surveying method where a single field of force or anomalous property (such as elasticity, magnetism, gravitation, or radioactivity) is used.

Electrical methods of geophysical investigations are based on the resistivity (or its inverse, conductivity) contrasts of subsurface materials. The electrical resistance R of a material is related to its physical dimension, cross-sectional area A, and length l through the resistivity ρ or its inverse, conductivity, by σ by

$$\rho = \frac{1}{\sigma} = \frac{RA}{l}. \tag{3}$$

Low-frequency alternating current is employed as source signals in the DC resistivity surveys in determining the subsurface resistivity distributions. Thus, the magnetic properties of the materials can be ignored [44, 45] so that Maxwell's equations of electromagnetism reduced to

$$\nabla \cdot \vec{E} = \frac{1}{\varepsilon_0} q, \tag{4}$$

$$\nabla \times \vec{E} = 0, \tag{5}$$

$$\vec{E} = -\nabla + \Phi, \tag{6}$$

where $\vec{E}$ is the electric field in V/m, q is the charge density in C/m^3, and ε_0 is the permittivity of free space ($\varepsilon_0 = 8.854 \times 10^{-12}$ F/m). These equations are applicable to continuous flow of direct-current; however, they can be used to represent the effects of alternating currents at low frequencies such that the displacement currents and induction effects are negligible.

4. Signal-to-Noise Ratio and Electromagnetic Coupling

Signal-to-noise ratio and electromagnetic coupling are other factors that influence the choice of an array. If a collinear electrode configuration is assumed, the signal-to-noise ratio of an array would depend on whether the potential electrodes are placed within or outside the current electrodes. The potential difference and the signal strength would be higher for potential electrodes placed within the current electrodes than those placed outside the current electrodes. The geometric factor of an array is indirectly related to its signal strength; it reflects the range of potential differences to be expected for a particular electrode configuration. Low values of geometric factor indicate that high potential difference would be observed and vice versa. This implies that electrode configurations with low geometric factor will yield high signal-to-noise ratio. Thus, electrode configurations with low geometric factor would be preferred if high signal-to-noise ratio is desired since a combination of high values of geometric factor with low voltage measurements may be overwhelmed with noise.

The frequencies of source signals in direct current geoelectrical resistivity surveys are usually very low. This ensures that electromagnetic effects are minimal. However, most commercial resistivity measuring instruments employ square waves or pulsed direct currents as source signals. The spectral analysis of such signals shows that they generate high

frequency harmonics which may result in electromagnetic coupling between the two dipoles (current electrodes and potential electrodes) and the connecting cables. Stability of the measured response can be ensured by choosing long cycle times of the input signal relative to the decay time. Other things being equal, electromagnetic coupling may be due to the following:

(i) increasing frequency of the input signal, a slowly varying sinusoidal signal would generally suppress coupling effects;

(ii) the sensitivity of the electrode configuration to coupling effects;

(iii) heterogeneities of the subsurface;

(iv) cultural effects arising from inductive coupling due to power lines, transmission lines, pipelines, buried cables, and so forth that may be close to the survey line.

5. Comparison of the Conventional Electrode Arrays

The conventional Wenner and Schlumberger arrays are relatively sensitive to vertical variations in the subsurface resistivity below the centre of the array but less sensitive to horizontal variations in the subsurface resistivity. The arrays have a moderate depth of investigation and generally strong signal strength which is inversely proportional to its geometric factor which is used in calculating the apparent resistivity. The major limitation of these arrays is the relatively poor horizontal coverage with increased electrode spacing. The Wenner array is preferred for surveys in a noisy site because of its high signal strength; however, the array is less sensitive to 3D structures.

The dipole-dipole array is the most sensitive to resistivity variations below the electrodes in each dipole pair and is very sensitive to horizontal variations but relatively insensitive to vertical variations in the subsurface resistivities. Thus, it is the most preferred array for mapping vertical structures like dykes and cavities. Dipole-dipole array is, however, very poor in mapping horizontal structures such as sills, sedimentary, or horizontal layers. Additionally, it is the most sensitive array to 3D structure among the common arrays [46]. The depth of investigation of the array depends on both the current electrode spacing and the distance between the two dipoles and is generally shallower than that of Wenner array. However, dipole-dipole array has better horizontal data coverage than Wenner array. The major disadvantage of this array is the decrease in signal strength with increasing distance between the dipole pair.

The pole-dipole array is an asymmetrical array with asymmetrical apparent resistivity anomalies in the pseudosections over a symmetrical structure, which could influence the inversion model. It has a relatively good horizontal coverage, and higher signal strength compared with dipole-dipole array. It is much less sensitive to telluric noise than the pole-pole array. Repeating measurements with the electrodes arranged in the reverse order can eliminate the asymmetrical effect. The combined measurements of the forward and reverse pole-dipole array would remove any bias in the model due to asymmetry [16]. However, this will increase the survey time as the number of data points to be measured will be doubled. The signal strength of the pole-dipole array is lower than that of Wenner and Schlumberger arrays and is very sensitive to vertical structures.

The pole-pole array consists of one current and one potential electrode with the second current and potential electrodes at infinite distances. Finding suitable locations for these electrodes so as to satisfy this theoretical requirement is often difficult. In addition to this limitation, the pole-pole array is highly susceptible to large amount of telluric noise capable of degrading the quality of the observed data. The array has the widest horizontal coverage and the deepest depth of investigation but the poorest resolution. The resolution of the pole-pole array is very poor as subsurface structures tend to be smeared out in the inversion model [16]. If the electrode spacing is small and good horizontal coverage is desired, the pole-pole array is a reasonable choice.

6. Data Acquisition Instruments

Geoelectrical resistivity field data are acquired using earth resistivity meter commonly referred to as Terrameter. The equipment is portable, light weight, and relatively cost effective when compared with other geophysical data acquisition systems. A conventional setup of the earth resistivity meter (Figure 4) basically consists of the following. The automated data acquisition systems generally consist of a resistivity instrument, a relay unit (electrode selector), a portable computer (commonly a laptop), electrode cables, various connectors, and electrodes [24, 47]. Two or more components of the multielectrode systems may be housed in the same box, making the systems more compact and portable. Some multielectrode systems employ intelligent switches at each electrode take-out instead of a central switching unit. The automated multielectrode systems are either single channel or multichannel. For any N-channel multielectrode systems, N numbers of data can be recorded simultaneously thereby increasing the data acquisition speed by a factor of N. The multichannel systems are also capable of measuring field data with a single channel if desired. A number of multielectrode systems are commercially available for near surface investigations, such as the SAS 4000 Lund (ABEM), Geo Tom (Geolog), Tomoplex (Campus Ltd), Super String R8 (AGI Inc), and RESECS (DTM GmbH).

In field surveys, the cables are rolled out along the survey line(s) as predesigned by the field crew and the electrodes are connected to the electrode take-outs which are usually numbered on the cables. Two to four cables may be used together in a given survey depending on the acquisition system and the electrode configuration used. The electrode take-out number should increase in the direction of increasing coordinate number. The acquisition systems automatically check the electrode contacts and scan through a predefined measurement protocol. The extension of the survey line can be achieved through roll-along technique (Figure 5) in which

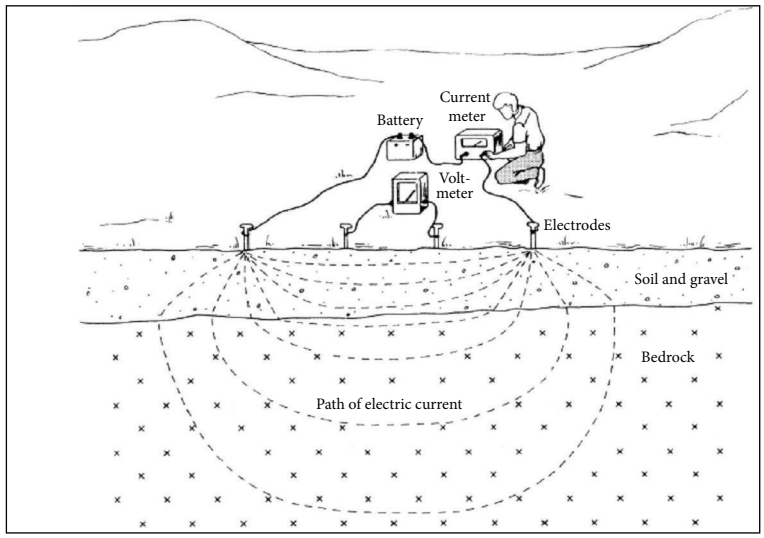

Figure 4: A schematic earth resistivity meter and field observation [48].

part of the layout is shifted along the survey so as to make new measurements in areas not already covered. The systems allow automatic updating of the coordinates in both x- and y-axes if roll-along technique is employed.

7. Types of Geoelectrical Resistivity Surveys

Geoelectrical resistivity surveys for delineating subsurface resistivity contrast may be classified as follows:

(i) vertical electrical sounding or electric drilling;

(ii) geoelectrical resistivity profiling (constant separation traversing);

(iii) two-dimensional (2D) geoelectrical resistivity imaging;

(iv) three-dimensional (3D) geoelectrical resistivity imaging.

7.1. Vertical Electrical Sounding (VES). In vertical electrical sounding (VES) or "electric drilling" [50], the centre point of the array remains fixed (fixed potential electrodes) but the current electrode separation is progressively increased. The Schlumberger array is mostly used for VES surveys because of its logistic simplicity; however, other configurations such as Wenner array with equal electrode spacing can be used. The vertical variation in the subsurface electrical resistivity at the point of investigation is obtained. The subsurface is assumed to consist of horizontally stratified layers in which the resistivity varies only with depth but not in the horizontal (or lateral) direction. Thus, the model of interpretation of VES is one-dimensional (1D) and is inherently insensitive to lateral variations in the subsurface resistivity, which may lead to significant changes in apparent resistivity values. These changes are often misinterpreted as changes in resistivity with depth. However, useful results have been obtained for geological situations such as depth to bedrock where the 1D model is approximately true.

The observed apparent resistivities are usually plotted against half-current electrode spacing on a double logarithm graphs. The resulting curves are then matched against theoretical model curves of typical subsurface resistivity structures commonly referred to as master curves, usually 2-layer curves. The presence of a turning point in the curves indicates a boundary (an interface) between two layers. The shape of the curves depends on the resistivity contrast between two layers. Sequences of several layers can be interpreted using auxiliary point diagrams. A variety of algorithms for numerical computation of apparent resistivity versus depth were developed in the 1960s and 1970s [50, 51]. This was followed by the development of forward modelling and inversion schemes that allowed the resistivity of layered models (1D) to be obtained on computers [52–54]. With the computer inversion schemes which are based on linear inverse theory, the covariance matrix of the inverse problem can be analysed.

For a horizontally stratified earth model which is homogeneous and isotopic, the potential and apparent resistivity distribution can easily be computed using recurrence formulas and linear filtering techniques.

7.2. Geoelectrical Resistivity Profiling. Constant separation traversing (CST) or profiling method is the second approach employed in classical resistivity surveys, where the electrode separation remains fixed both in dimension and in orientation. The entire array is progressively moved along a straight line usually in the direction perpendicular to the geologic strike. This gives lateral variations in the subsurface resistivity at an approximate constant depth and is incapable of detecting vertical variations in the subsurface resistivity. Data obtained from profiling are mainly interpreted qualitatively. The Wenner configuration is best suited for this approach due to the equidistant spacing between the electrodes. For

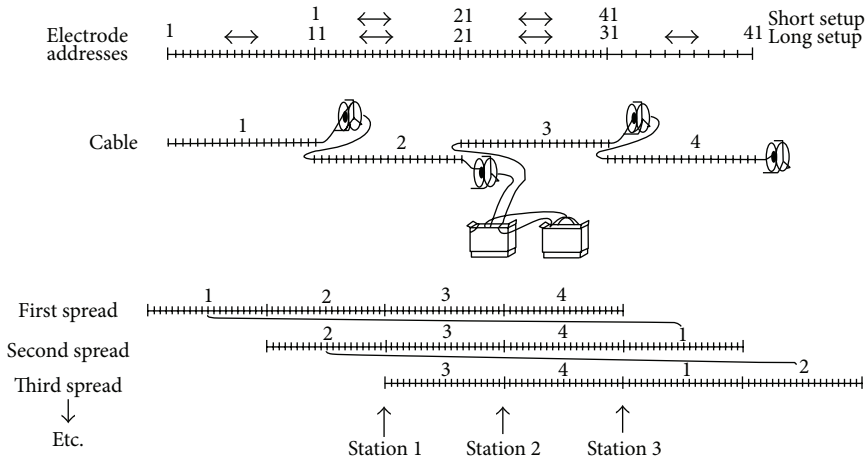

Figure 5: Roll-along technique using four electrode cables [49].

special problems, such as the determination of a steeply dipping structure or the precise determination of a fault, the dipole-dipole array is preferred. Generally, the gradient array could be a good choice in electrical resistivity profiling because only the potential electrodes need to be moved [55]. Usually, a completely homogeneous and isotropic earth medium of uniform resistivity is assumed. For a continuous current flowing in an isotropic and homogeneous medium, the current density $\vec{J}$ is related to the electric field $\vec{E}$ through Ohm's law:

$$\vec{J} = \sigma \vec{E}. \tag{7}$$

The electric field vector $\vec{E}$ can be represented as the gradient of the electric scalar potential:

$$\vec{E} = -\nabla \Phi. \tag{8}$$

Thus, the current density $\vec{J}$ becomes

$$\vec{J} = -\sigma \nabla \Phi. \tag{9}$$

By combining (4) and (6), we obtain the fundamental Poisson equation for electrostatic fields given by

$$\nabla^2 \Phi(x, y, z) = -\frac{1}{\varepsilon_0} q(x, y, z). \tag{10}$$

The equation of continuity for a point in 3D space and time t defined by the Dirac delta function is given as

$$\nabla \cdot \vec{J}(x, y, z, t) = -\frac{\delta}{\delta t} q(x, y, z, t)\, \delta(x)\, \delta(y)\, \delta(z). \tag{11}$$

The current sources in a typical electrical resistivity survey are usually point sources. Thus, the current and the current density over a volume element ΔV around a current source I located at (x, y, z) are given by the relation [56] as

$$\nabla \cdot \vec{J} = \left(\frac{I}{\Delta V}\right) \delta(x - x_s)\, \delta(y - y_s)\, \delta(z - z_s), \tag{12}$$

where δ is the Dirac delta function. Hence, the potential distribution in the ground due to a point current source is

$$\begin{aligned} \nabla \cdot \vec{J} &= \left[\sigma(x, y, z)\, \nabla \Phi(x, y, z)\right] \\ &= \left(\frac{I}{\Delta V}\right) \delta(x - x_s)\, \delta(y - y_s)\, \delta(z - z_s). \end{aligned} \tag{13}$$

This partial differential equation, which is a self-adjoint, strongly connected, and nonseparable elliptic equation of second order [57], gives the subsurface potential distribution in an isotropic nonuniform 3D medium due to a point current source. Numerous techniques have been developed to solve this problem, that is, to determine the potential distribution that would be observed over a given subsurface structure. The potential $\Phi(x, y, z)$ and the normal component of the current density $\sigma \delta \Phi / \delta n$ are continuous across the boundary between two media of different resistivities but the current lines are refracted in accordance with the boundary conditions.

8. Potential Distribution due to Point Source in a Homogeneous Half-Space

All resistivity methods employ an artificial source of current injected into the subsurface through point electrodes and the resulting potential difference is measured at other electrode positions in the neighbourhood of the current flow. For a semi-infinite conducting layer of uniform resistivity (a completely homogeneous and isotropic medium) bounded by the ground surface as shown in Figure 6 a current of strength $+I$ is injected at a point C_1 into the ground surface. This current will flow away radially from the point of entering and its distribution will be uniform over a hemispherical shell of an underground region (Figure 7) of resistivity ρ. The potential varies inversely with the distance from the current source. The currents flow and the equipotential surfaces are perpendicular. At a distance r of a point in the medium from the point source, the surface area of the hemispherical shell is $2\pi r^2$ so that the current density $\vec{J}$ becomes $I/2\pi r^2$.

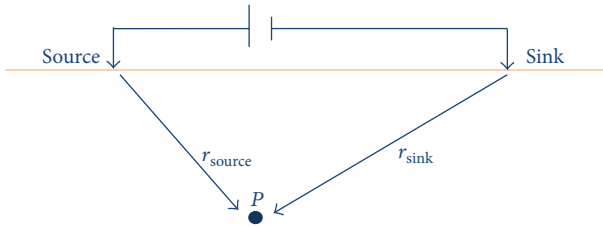

FIGURE 6: A diagram showing a homogenous and isotropic medium.

Thus, the potential for the homogeneous half-space is

$$\Phi(r) = \frac{PI}{2\pi r}. \quad \text{(i)}$$

In practice, two current electrodes, the current source $+I$ and the sink $-I$ (Figure 6), are often used. The potential distribution is symmetrical about the vertical placed at the midpoint between the two current electrodes. The potential at an arbitrary point from a given pair of current electrodes, by applying (i), is obtained as

$$\Phi(r) = \frac{PI}{2\pi}\left(\frac{1}{{}^{r}C_1} - \frac{1}{{}^{r}C_2}\right), \quad \text{(ii)}$$

where ${}^{r}C_1$ and ${}^{r}C_2$ are the respective distances from the first (source) and second (sink) current electrode to the arbitrary point.

9. Apparent Resistivity and Geometric Factor

Usually, the potential difference between two points is measured. The injecting (current) electrodes could be used, in theory, to measure the potential difference. But the influence of the resistances between the subsurface and current electrodes is not precisely known [58]. Thus, two potential electrodes are dedicated to detect the response signal. If P_1 and P_2 are the potential electrodes, the potential difference between P_1 and P_2 is shown in Figure 3.

10. Modelling and Inversion Techniques

The numerical modelling and inversion techniques employed in different geological conditions usually encountered in geophysical application for environmental, hydrogeological, and engineering investigations in tropical regions are numerically studied. A net of parallel and perpendicular 2D model structures was approximated from these 3D synthetic models. Apparent resistivity values were then calculated over the resulting 2D synthetic models for the following arrays: Wenner-alpha, Wenner-beta, Wenner-Schlumberger, dipole-dipole, pole-dipole, and pole-pole arrays. The apparent resistivity values were calculated for different minimum electrode spacings and interline spacings over the same models. In addition, the apparent resistivity values that would be observed over the synthetic models if rectangular or square grids of electrodes are used for the survey were computed for the different arrays except for Wenner-beta, which is basically a dipole-dipole array with a dipole separation equal to the dipole length, using the different minimum electrode separations considered.

It is usually recommended that apparent resistivity values for the parallel and perpendicular sets of 2D profiles over the synthetic model for each of the arrays under consideration should be collated into 3D data sets. More so, the electrode arrays should be paired such that the apparent resistivity of all parallel 2D profiles must be computed with the same array and those in a perpendicular direction are computed with the second array that makes the pair. Inversions of the collated 3D data sets as well as the 3D data sets calculated using RES3DMOD were usually carried out using a three-dimensional inversion code (RES3DINV) that allows the variation of model resistivity values in all directions. The smoothness constrained and robust inversion methods are used separately on the same data sets so as to evaluate their relative effectiveness in 3D inversion. Among the various electrode arrays considered, the dipole-dipole and pole-dipole arrays generally yield higher anomaly effects while Wenner-Schlumberger array produced moderate anomaly effect on the synthetic models. In both synthetic models, pole-pole array yields the least anomaly effects.

The normalized average sensitivity model values of dipole-dipole and pole-dipole are much higher than those of other arrays and Wenner-Schlumberger array yields a moderate model sensitivity values. This indicates that dipole-dipole and pole-dipole arrays are more sensitive to 3D features and thus would yield better resolution of 3D inversion models. The Wenner-Schlumberger array may be a good compromise between the high sensitivity dipole-dipole and pole-dipole arrays and the low sensitivity pole-pole, Wenner-alpha, and Wenner-beta arrays in terms of inversion model sensitivity and resolution. The sensitivity and resolution of the arrays to 3D features were found to generally improve for orthogonal paired arrays.

11. Sensitivity and Resolution

In geoelectrical resistivity imaging, the imaging capabilities of different electrode configurations are different when applied to a particular geologic structure. These differences in imaging capability are often reflected in the spatial resolution of the arrays, the tendency of the array to produce artefacts in the resulting model inversion images, deviations from the true resistivity model values, and the maximum depth of investigations attained by the arrays. To obtain reliable and high-resolution images in geoelectrical resistivity imaging, the electrode configuration used in the measurements should ideally give data with maximum anomaly information, reasonable data coverage, and high-signal to noise ratio. In theory a complete data set of an array with minimum noise contamination is required to obtain such a high-resolution image. But acquiring such large number of data points would significantly increase the time required for the field measurements even when automatic data acquisition systems are used. A large number of data points could also make it difficult for the inversion to attain a good data misfit and

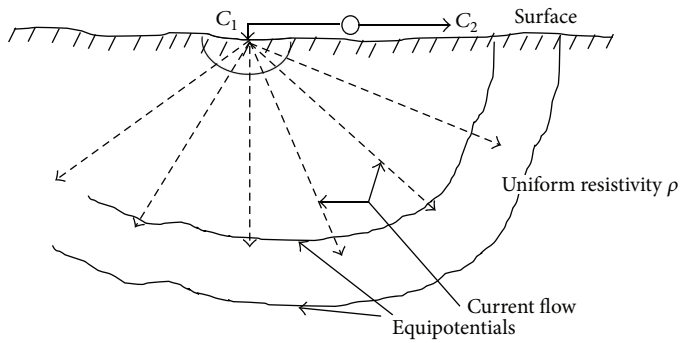

Figure 7: Current from a point source and the resulting equipotential distribution.

probably produce more artefacts in the inversion images due to the unknown characteristics of the noise contamination in the data.

Generally the overall sensitivity of the image plane decreases rapidly with depth, indicating a significant loss of resolution with depth.

The average model sensitivities observed in dipole-dipole and pole-dipole arrays are much higher than those in the other arrays investigated. This implies that dipole-dipole and pole-dipole arrays, using combination of 2D profiles, are more sensitive to 3D features than any of the conventional arrays investigated. The observed high model sensitivity values for dipole-dipole and pole-dipole arrays are in agreement with the high anomaly effects calculated for these arrays. In general, pole-pole and Wenner-beta arrays showed the least sensitivity in all the inversion models tested. This is partly due to the fact that these arrays have the highest depth of investigation under similar conditions with other arrays and sensitivity generally decreases with depth. The Wenner-Schlumberger array shows moderate sensitivity values and thus may be a good compromise between the more sensitive dipole-dipole and pole-pole arrays and the less sensitive arrays for 3D survey.

The sensitivity pattern of an electrode array is an important factor in the determination of its imaging capability. Each apparent resistivity measurement, usually made with a unique set of four electrodes, can be viewed as a weighted sum of the distributed electrical resistivity within a volume sampled by the set of four electrodes. The best-fit of the electrical resistivity distribution can be determined by simultaneous inversion of large number of apparent resistivity measurements made with overlapping sampled volumes. The sampled volume and the manner in which the distributed electrical resistivities are weighted depend on the locations and the configuration of the electrodes used for the measurements. The spatial sensitivity distribution of each set of four-electrodes used for the measurements accumulates to define the spatial sensitivity of the entire survey.

The sensitivity of a set of four electrodes can be defined as the change in potential measured with the potential electrodes because of given change in the subsurface conductivity (or resistivity) in a small area located at (x, y). An equivalent form can be written in terms of the apparent resistivity. The sensitivity of the set of four electrodes can be calculated for many locations throughout the subsurface to produce a map of spatial sensitivity. The sensitivity provides information on the section of the subsurface with the greatest effect on the measured apparent resistivity.

12. Factors Affecting Sensitivity and Resolution

The following are some of the factors that could influence the sensitivity and resolution of 3D inversion in geoelectrical resistivity imaging:

(i) Data Density and Lateral Coverage. The sensitivity of geoelectrical resistivity increases with increasing data density relative to the grid size of the electrodes. The higher the lateral data coverage of an electrode array the greater the model sensitivity values that would be obtained in the inversion.

(ii) Depth of Penetration. The sensitivity of electrical resistivity of the subsurface for a given electrode configuration generally decreases with depth of investigation. Thus, electrode configurations with greater depth of penetration are largely less sensitive than those with less depth of penetration for the same data level.

(iii) Damping Factor and Noise Contamination. The choice of the damping parameters for a particular data set also affects the overall sensitivity of the resulting model resistivity values. Appropriate damping factor that would yield the optimum sensitivity can be selected through trial and error method, or with experience based on the knowledge of the geology. Noisy data generally require a higher damping factor than less noisy data. Some arrays are more sensitive to noise than others; the sensitivity of the arrays to noise contaminations can significantly affect the sensitivity of the inversion models.

(iv) Inter-line Spacing and Electrodes Grid Size. In the case of 3D geoelectrical resistivity imaging using orthogonal or parallel 2D profiles, the interline spacing relative to the minimum electrode separation can significantly affect the overall sensitivity of the resulting inversion models. In theory, the interline spacing should be the same with the minimum electrode separation; this may not be practical considering

the volume of work and time required for field data measurements. Electrode grid sizes with regular or uniform electrode spacing in both directions are found to yield higher sensitivity values than corresponding grid sizes with irregular electrode spacing.

(v) Geological Conditions. The nature of the subsurface geology, geometry of subsurface features, and the electrical properties (or resistivity contrast) of the anomalous body can also significantly influence the overall sensitivity of the inversion models.

The sensitivity values of electrode configurations provide information on the section of the subsurface with the greatest effect on the measured apparent resistivity values. In geoelectrical resistivity imaging, the sensitivity is a very important and indicative property in the interpretation process. Generally, the spatial sensitivity patterns for homogeneous environments are good approximations for moderate conductivity/resistivity contrasts not exceeding 1 : 10 if the source is located within conductive material [39].

13. Conclusion

Pole-dipole and pole-bipole have moderate anomaly effects and relatively low signal to noise ratio, and both can yield better spatial resolution images than those of pole-pole, Schlumberger, and Wenner. Increasing potential electrodes enhances spatial resolution and better signal to noise ratio and thus reducing noise contamination. One remote electrode accessibility of surveys complicates data quality by reciprocal measurements since the noise from the remote potential electrode can be higher. Wenner and Schlumberger have similarity and resemblance in electric field measurements due to their imaging abilities with their main strength in depth determination in comparison to other electrodes. However, Wenner has poorer spatial resolution than that of pole-dipole, pole-bipole, dipole-dipole, and Schlumberger arrays, while Schlumberger with reduction of the signal to noise ratio, may offer improved imaging resolution side by side with Wenner but may pick up noise than the normal array when assessing the data quality using reciprocal measurements. Dipole-dipole has relatively high anomaly effects and risk of noise contamination but often produces low signal to noise ratio in surveys when compared with Wenner-beta, Wenner, and gamma arrays. Gamma array has advantage of low noise contamination of imaging survey in all arrays, but the signal-to-noise ratio and anomaly effects are consistently high, and spatial resolution of the imaging is not as good as the other arrays. Gradient array has good spatial resolution while midpoint-potential-referred has higher signal-to-noise ratio with lower spatial resolution in the image. Midpoint potential referred has an option for multichannel recording array due to its lower noise sensitivity. The square-array is more sensitive to a given rock heterogeneity and anisotropy than the more commonly used Schlumberger and Wenner arrays.

References

[1] P. A. Ahzegbobor, *Acquisition geometry and inversion of 3D geoelectrical resistivity imaging data for environmental and engineering investigations [Ph.D. thesis]*, Physics Department, Covenant University, Ota, Nigeria, 2010.

[2] R. D. Barker, "Signal contribution sections and their use in resistivity studies," *Geophysical Journal*, vol. 59, no. 1, pp. 123–129, 1979.

[3] M. Muskat and H. H. Evinger, "Current penetration in direct current prospecting," *Geophysics*, vol. 6, pp. 397–427, 1941.

[4] H. M. Evjen, "Depth factor and resolving power of electrical measurements," *Geophysics*, vol. 3, pp. 78–85, 1938.

[5] A. Roy and A. Apparao, "Depth of investigation in direct current methods," *Geophysics*, vol. 36, pp. 943–959, 1971.

[6] A. Roy, "Depth of investigation in Wenner, three-electrode and dipole-dipole DC resistivity methods," *Geophysical Prospecting*, vol. 20, no. 2, pp. 329–340, 1972.

[7] O. Koefoed, "Discussion on "Depth of investigation in direct current methods" by A. Roy and A. Apparao," *Geophysics*, vol. 37, pp. 703–704, 1972.

[8] D. S. Parasnis, "More comments on "A theorem for Dc regimes and some of its consequences" by A. Roy," *Geophysical Prospecting*, vol. 32, pp. 139–141, 1984.

[9] S. C. Guerreiro, "Comment on "A theorem for direct current regimes and some of its consequences" by A. Roy and some related papers and comments," *Geophysical Prospecting*, vol. 31, no. 1, pp. 192–195, 1983.

[10] B. Banerjee and B. P. Pal, "A simple method for determination of depth of investigation characteristics in resistivity prospecting," *Exploration Geophysics*, vol. 17, pp. 93–95, 1986.

[11] M. N. Nabighian and C. L. Elliot, "Negative induced polarization effects from layered media," *Geophysics*, vol. 41, no. 6, pp. 1236–1255, 1976.

[12] K. K. Roy and H. M. Elliot, "Some observations regarding depth of exploration in D.C. electrical methods," *Geoexploration*, vol. 19, no. 1, pp. 1–13, 1981.

[13] L. S. Edwards, "A modified pseudosection for resistivity and induced polarization," *Geophysics*, vol. 42, no. 5, pp. 1020–1036, 1977.

[14] R. D. Barker, "Depth of investigation of collinear symmetrical four-electrode arrays," *Geophysics*, vol. 54, no. 8, pp. 1031–1037, 1989.

[15] T. Dahlin and B. Zhou, "A numerical comparison of 2D resistivity imaging with 10 electrode arrays," *Geophysical Prospecting*, vol. 52, no. 5, pp. 379–398, 2004.

[16] M. H. Loke, "Tutorial: 2D and 3D electrical imaging surveys," 2004, http://www.geotomosoft.com/.

[17] O. Pazdirek and V. Blaha, "Examples of resistivity imaging using ME-100 resistivity field acquisition system," in *Proceedings of the EAGE 58th Conference and Technical Exhibition Extended Abstracts*, Amsterdam, The Netherlands, 1996.

[18] M. H. Loke, "Electrical Imaging surveys for environmental and engineering studies: a practical guide to 2D and 3D surveys," 2001, http://www.geotomosoft.com/.

[19] P. Stummer, H. Maurer, and A. G. Green, "Experimental design: electrical resistivity data sets that provide optimum subsurface information," *Geophysics*, vol. 69, no. 1, pp. 120–139, 2004.

[20] P. B. Wilkinson, P. I. Meldrum, J. E. Chambers, O. Kuras, and R. D. Ogilvy, "Improved strategies for the automatic selection of optimized sets of electrical resistivity tomography measurement

configurations," *Geophysical Journal International*, vol. 167, no. 3, pp. 1119–1126, 2006.

[21] A. Furman, T. P. A. Ferré, and G. L. Heath, "Spatial focusing of electrical resistivity surveys considering geologic and hydrologic layering," *Geophysics*, vol. 72, no. 2, pp. F65–F73, 2007.

[22] T. Hennig, A. Weller, and M. Möller, "Object orientated focussing of geoelectrical multielectrode measurements," *Journal of Applied Geophysics*, vol. 65, no. 2, pp. 57–64, 2008.

[23] J. Chambers, R. Ogilvy, P. Meldrum, and J. Nissen, "3D resistivity imaging of buried oil- and tar-contaminated waste deposits," *European Journal of Environmental and Engineering Geophysics*, vol. 4, no. 1, pp. 3–14, 1999.

[24] T. Dahlin, *On the Automation of 2D Resistivity Surveying for Engineering and Environmental Applications*, Lind University, 1993.

[25] Y. Sasaki, "Resolution of resistivity tomography inferred from numerical simulation," *Geophysical Prospecting*, vol. 40, no. 4, pp. 453–463, 1992.

[26] T. Dahlin and M. H. Loke, "Resolution of 2D Wenner resistivity imaging as assessed by numerical modelling," *Journal of Applied Geophysics*, vol. 38, no. 4, pp. 237–249, 1998.

[27] A. I. Olayinka and U. Yaramanci, "Assessment of the reliability of 2D inversion of apparent resistivity data," *Geophysical Prospecting*, vol. 48, no. 2, pp. 293–316, 2000.

[28] H. Militzer, R. Rosler, and W. Losch, "Theoretical and experimental investigations for cavity research with geoelectrical resistivity methods," *Geophysical Prospecting*, vol. 27, no. 3, pp. 640–652, 1979.

[29] G. M. Habberjam, "Apparent resistivity anisotropy and strike measurements," *Geophysical Prospecting*, vol. 23, no. 2, pp. 211–247, 1975.

[30] G. M. Habberjam, "The effects of anisotropy on square array resistivity measurements," *Geophysical Prospecting*, vol. 20, no. 2, pp. 249–266, 1972.

[31] R. G. Van Nostrand and K. L. Cook, "Interpretation of resistivity data," U. S. Geological Survey Professional, 499 pages, 1966, http://books.google.com/.

[32] K. Spitzer and H.-J. Kümpel, "3D FD resistivity modelling and sensitivity analyses applied to a highly resistive phonolitic body," *Geophysical Prospecting*, vol. 45, no. 6, pp. 963–982, 1997.

[33] P. R. McGillivray and D. W. Oldenburg, "Methods for calculating Frechet derivatives and sensitivities for the non-linear inverse problem: a comparative study," *Geophysical Prospecting*, vol. 38, no. 5, pp. 499–524, 1990.

[34] D. E. Boerner and G. F. West, "Frechet derivatives and single scattering theory," *Geophysical Journal International*, vol. 98, no. 2, pp. 385–390, 1989.

[35] D. W. Oldenburg, "The interpretation of direct current measurements," *Geophysics*, vol. 43, no. 3, pp. 610–625, 1978.

[36] Y. Sasaki, "3-D resistivity inversion using the finite-element method," *Geophysics*, vol. 59, no. 12, pp. 1839–1848, 1994.

[37] M. Noel and B. X. Biwen Xu, "Archaeological investigation by electrical resistivity tomography: a preliminary study," *Geophysical Journal International*, vol. 107, no. 1, pp. 95–102, 1991.

[38] S. K. Park and G. P. Van, "Inversion of pole-pole data for 3-D resistivity structure beneath arrays of electrodes," *Geophysics*, vol. 56, no. 7, pp. 951–960, 1991.

[39] K. Spitzer, "The three-dimensional DC sensitivity for surface and subsurface sources," *Geophysical Journal International*, vol. 134, no. 3, pp. 736–746, 1998.

[40] J. A. Stratton, *Electromagnetic Theory*, McGraw-Hill, New York, NY, USA, 1941.

[41] R. F. Harrinton, *Harmonic Electromagnetic Fields*, Electrical and Electronic Engineering Series, McGraw-Hill, New York, NY, USA, 1961.

[42] F. S. Grant and G. F. West, *Interpretation Theory in Applied Geophysics*, McGraw-Hill, New York, NY, USA, 1965.

[43] S. H. Ward and G. W. Hohmann, "Electromagnetic theory for geophysical applications," in *Electromagnetic Methods in Applied Geophysics, Investigations in Geophysical Series*, M. N. Nabighian, Ed., vol. 1, pp. 131–312, Society of Exploration Geophysicists, Tulsa, Okla, USA, 1987.

[44] G. V. Keller and F. C. Frischknecht, *Methods in Geophysical Prospecting*, Pergamo Press, 1966.

[45] W. M. Telford, L. P. Geldart, R. E. Sheriff, and D. A. Keys, *Applied Geophysics*, Cambridge University Press, Lodon, UK, 1976.

[46] T. Dahlin and M. H. Loke, "Quasi-3D resistivity imaging-mapping of three-dimensional structures using two-dimensional DC resistivity techniques," in *Proceedings of the 3rd Meeting of the Environmental and Engineering Geophysical Society*, pp. 143–146, 1997.

[47] D. H. Griffiths, J. Turnbull, and A. I. Olayinka, "Two-dimensional resistivity mapping with a complex controlled array," *First Break*, vol. 8, no. 4, pp. 121–129, 1990.

[48] E. S. Robinson and C. Coruh, *Exploration Geophysics*, John Wiley & Sons, New York, NY, USA, 1988.

[49] R. A. V. Overmeeren and I. L. Ritsema, "Continuous vertical electrical sounding," *First Break*, vol. 6, no. 10, pp. 313–324, 1988.

[50] O. Koefoed, *Geosounding Principles 1: Resistivity Sounding Measurements*, Elsevier Science, Amsterdam, The Netherlands, 1979.

[51] H. M. Mooney, E. Orellana, H. Pickett, and L. Tornheim, "A resistivity computation method for layered earth models," *Geophysics*, vol. 31, pp. 192–203, 1966.

[52] D. P. Ghosh, "The application of linear filter theory to the direct interpretation of geoelectrical resistivity sounding measurements," *Geophysical Prospecting*, vol. 19, pp. 192–217, 1971.

[53] J. R. Inman, J. Ryu, and S. H. Ward, "Resistivity inversion," *Geophysics*, vol. 38, no. 6, pp. 1088–1108, 1973.

[54] A. A. R. Zohdy, "A new method for the automatic interpretation of Schlumberger and Wenner sounding curves," *Geophysics*, vol. 54, no. 2, pp. 245–253, 1989.

[55] P. Furness, "Gradient array profiles over thin resistive veins," *Geophysical Prospecting*, vol. 41, no. 1, pp. 113–130, 1993.

[56] A. Dey and H. F. Morrison, "Resistivity modelling for arbitrarily shaped three- dimensional structure," *Geophysics*, vol. 44, no. 4, pp. 753–780, 1979.

[57] R. S. Varga, *Matrix Iteration Analysis*, Prentice-Hall, Englewood Cliffs, NJ, USA, 1962.

[58] K. S. Cheng, S. J. Simske, D. Isaacson, J. C. Newell, and D. G. Gisser, "Errors due to measuring voltage on current-carrying electrodes in electric current computed tomography," *IEEE Transactions on Biomedical Engineering*, vol. 37, no. 1, pp. 60–65, 1990.